

1 **Downscaling Satellite Soil Moisture using Geomorphometry and**  
2 **Machine Learning**

3

4 Authors:

5 Mario Guevara<sup>1</sup> and Rodrigo Vargas<sup>1\*</sup>

6 <sup>1</sup>University of Delaware, Department of Plant and Soil Sciences, Newark, DE, 19716

7 \*Corresponding author

8 E-mail: [rvargas@udel.edu](mailto:rvargas@udel.edu)

9

10

11

## 12 **Abstract**

13 Annual soil moisture estimates are useful to characterize trends in the climate system, in the capacity of  
14 soils to retain water and for predicting land and atmosphere interactions. The main source of soil  
15 moisture spatial information across large areas (e.g., continents) is satellite-based microwave remote  
16 sensing. However, satellite soil moisture datasets have coarse spatial resolution (e.g., 25-50 km grids);  
17 and large areas from regional-to-global scales have spatial information gaps. We provide an alternative  
18 approach to predict soil moisture spatial patterns (and associated uncertainty) with higher spatial  
19 resolution across areas where no information is otherwise available. This approach relies on  
20 geomorphometry derived terrain parameters and machine learning models to improve the statistical  
21 accuracy and the spatial resolution (from 27km to 1km grids) of satellite soil moisture information  
22 across the conterminous United States on an annual basis (1991-2016). We derived 15 primary and  
23 secondary terrain parameters from a digital elevation model. We trained a machine learning algorithm  
24 (i.e., kernel weighted nearest neighbors) for each year. Terrain parameters were used as predictors and  
25 annual satellite soil moisture estimates were used to train the models. The explained variance for all  
26 models-years was >70% (10-fold cross-validation). The 1km soil moisture grids (compared to the  
27 original satellite soil moisture estimates) had higher correlations with field soil moisture observations  
28 from the North American Soil Moisture Database (n=668 locations with available data between 1991-  
29 2013; 0-5cm depth) than the original product. We conclude that the fusion of geomorphometry  
30 methods and satellite soil moisture estimates is useful to increase the spatial resolution and accuracy of  
31 satellite-derived soil moisture. This approach can be applied to other satellite-derived soil moisture  
32 estimates and regions across the world.

33

- 34 Keywords: Geomorphometry; terrain parameters; machine learning; satellite soil moisture;  
35 downscaling; uncertainty.

## 36 **Introduction**

37           Continuous national to continental scale soil moisture information is increasingly needed to  
38 characterize spatial and temporal trends of terrestrial productivity patterns (e.g., production of food,  
39 fiber and energy). This is because soil moisture is a key variable regulating hydrological and  
40 biogeochemical cycles, and thus studying its spatial-temporal dynamics is crucial for assessing the  
41 potential impact of climate change on water resources [1-4]. Currently, the most feasible way to obtain  
42 national to continental soil moisture information is using remote sensing. Microwave remote sensing  
43 devices deployed on multiple earth observation satellites are able to quantify the dielectric constant of  
44 soil surface and retrieve soil moisture estimates [5]. However, there are spatial gaps of satellite-based  
45 soil moisture information and its current spatial resolution (> 1km grids) limits its applicability at the  
46 ecosystem-to-landscape scales to address the ecological implications of soil moisture dynamics [5-8].

47           Satellite soil moisture records are an effective indicator for monitoring global soil conditions  
48 and forecasting climate impacts on terrestrial ecosystems, because soil moisture estimates are required  
49 for assessing feedbacks between water and biogeochemical cycles [9-12]. In addition, accurate soil  
50 moisture information is critical to predict terrestrial and atmospheric interactions such as water  
51 evapotranspiration or CO<sub>2</sub> emissions from soils [3, 13-15]. However, soil moisture information at  
52 spatial resolution of 1x1km pixels or less is not yet available across large areas of the world and the  
53 coarse pixel size (>1km pixels) of available satellite soil moisture records is limited for spatial analysis  
54 (i.e., hydrological, ecological) at small regional levels (e.g., county- to state). In addition, satellite soil  
55 moisture estimates are representative only of the first few 0-5 to 10 cm of top-soil surface [16].  
56 Therefore, comparing multiple sources for satellite soil moisture and field soil moisture estimates is  
57 constantly required for precise interpretations of soil moisture spatial patterns [17-19].

58           There is a pressing need for exploring statistical relationships across different sources of remote  
59 sensing information (e.g., topography and soil moisture) and developing alternative soil moisture  
60 spatial datasets (i.e., grids) to improve the continental-to-global spatial representation of soil moisture  
61 estimates [7]. Spatially explicit soil moisture estimates can be obtained across large areas with a spatial  
62 resolution between 25-50 km grids from radar-based microwave platforms deployed across different  
63 satellite soil moisture missions [20-21]. The availability of historical soil moisture records of these  
64 sources has increased during the last decade with unprecedented levels of temporal resolution (i.e.,  
65 daily from years 1978-present) at the global scale. However, large areas constantly covered by snow,  
66 extremely dry regions or tropical rain forests (where there is a higher content of water above ground)  
67 lack of precise soil moisture satellite records due to sensor intrinsic limitations (e.g., saturation or  
68 noise) across these environmental conditions [22].

69           One valuable product that is affected by the aforementioned environmental conditions is the  
70 ESA-CCI (European Space Agency Climate Change Initiative) soil moisture product [20-21]. The  
71 ESA-CCI mission makes rapidly available long-term soil moisture estimates with daily temporal  
72 resolution from the 1978s to date, and it represents the state-of-the-art knowledge tool for assessing  
73 long term trends in the climate system. Modeling, validation and calibration frameworks are required  
74 for improving the spatial representation of this important dataset, and for predicting soil moisture  
75 patterns across areas where no satellite estimates are available.

76           Currently, there is an increasing availability of fine-gridded information sources and modeling  
77 approaches that could be used for increasing the spatial resolution (hereinafter downscaling) of the  
78 ESA-CCI satellite soil moisture estimates (e.g., soil moisture predictions across <1x1km grids).  
79 Downscaling (and subsequently gap-filling) satellite soil moisture estimates has been the objective of  
80 empirical modeling approaches based on sub-grids of soil moisture related information such as soil

81 texture [23]. Other approaches followed environmental correlation methods and generated soil moisture  
82 predictions for satellite soil moisture estimates using both data-driven or hypothesis driven models and  
83 multiple sub-grids of ancillary information [24-26]. These sub-grids of information usually include  
84 vegetation related optical remote sensing imagery, gridded soil information, land cover classes and  
85 landforms [27-30]. Most of these approaches have been tested for specific study sites. Other studies  
86 have focused on applying a digital soil mapping approach (a reference framework for understanding the  
87 spatial distribution of soil variability [31]) and multiple upscaling methods for predicting soil moisture  
88 patterns at the continental scale [26, 32]; and an overview of multiple approaches for downscaling  
89 satellite soil moisture (e.g., empirically based, physically based) has been previously discussed [33].  
90 Here, we propose that digital terrain analysis (i.e., geomorphometry) can also be applied for empirically  
91 downscaling soil moisture satellite-based information across continental-to-global spatial scales.

92         Geomorphometry is an emergent discipline in earth sciences dedicated to the quantitative  
93 analysis of land surface characteristics and topography [34-35]. Topography includes a diversity of  
94 hydrologically meaningful terrain parameters (i.e., slope, aspect, curvature) that aim to represent how  
95 the landscape physically constrains water inputs (e.g., rainwater, irrigation, overland flow) that reaches  
96 the soil surface [35-36]. At the landscape scale, soil moisture is partially controlled by topography  
97 related factors (i.e., slope, aspect, curvature) physically constraining soil water inputs and soil hydraulic  
98 properties (e.g., soil texture, structure). Based on these geomorphometry principles [35-39], we propose  
99 that it is possible to determine which terrain parameters are the strongest predictors of the spatial  
100 variability of satellite soil moisture. Statistically coupling the spatial variability of satellite soil moisture  
101 with hydrologically meaningful terrain parameters could be an alternative way to improve the spatial  
102 resolution and accuracy of satellite soil moisture estimates across the continental scale. This is possible

103 because topography (represented by terrain parameters) directly affects: 1) the angle of the satellite  
104 microwave signal at the soil surface; and 2) the overall distribution of water in the landscape.

105 Topography is a major driver for soil moisture and topography surrogates (e.g., land form or  
106 elevation map) have been combined with other variables (e.g., climate, soils, vegetation and land use)  
107 for downscaling satellite soil moisture estimates [33]. However, the exclusive use of geomorphometry-  
108 derived products for downscaling satellite soil moisture has not yet been explored from national-to-  
109 continental scales. This approach is relevant to avoid statistical redundancies and potential spurious  
110 correlations when downscaled soil moisture is further used or analyzed with vegetation- or climate-  
111 related variables (when these aforementioned variables were used for downscaling of satellite derived  
112 soil moisture). In this study, we show the potential of a soil moisture prediction framework purely  
113 based on geomorphometry derived products (digital terrain parameters).

114 Our main objective is to generate a soil moisture prediction framework by coupling satellite soil  
115 moisture estimates with hydrologically meaningful terrain parameters as prediction factors. Coupling  
116 the complexity of topographic gradients and the multi-temporal nature of satellite soil moisture requires  
117 an approach that should account for non-linear relationships. Machine learning approaches could  
118 account for non-linearity based on probability and the ability of computer systems to reproduce and  
119 ‘learn’ (i.e., decide the best solution after multiple model realizations) from multiple modeling outputs  
120 (i.e., varying model parameters of combinations of training and testing random samples) [40].  
121 Furthermore, machine learning is now a common component of geoscientific research leading the  
122 discovery of new knowledge in the earth system [41] including soil greenhouse gas fluxes [8, 42] and  
123 soil moisture estimates [43].

124 We postulate that the data fusion between satellite soil moisture with hydrologically meaningful  
125 terrain parameters can enhance the spatial resolution, representativeness and quality (i.e., accuracy) of

126 current coarse satellite soil moisture grids. We focus on the conterminous United States (CONUS)  
127 given the large availability of soil moisture records for validating purposes from the North American  
128 Soil Moisture Database (NASMD) [44]. This study provides insights for obtaining detailed soil  
129 moisture estimates relying on public sources of satellite information and a data-driven framework that  
130 could be reproduced and applied across the world. The novelty of this research relies on proposing an  
131 alternative approach for obtaining soil moisture gridded measurements across areas where no soil  
132 moisture information is available (i.e., from the ESA-CCI) and at a spatial resolution (i.e., 1km)  
133 determined by the topographic prediction factors. This approach can be applied to other satellite-  
134 derived soil moisture estimates and regions across the world.

135

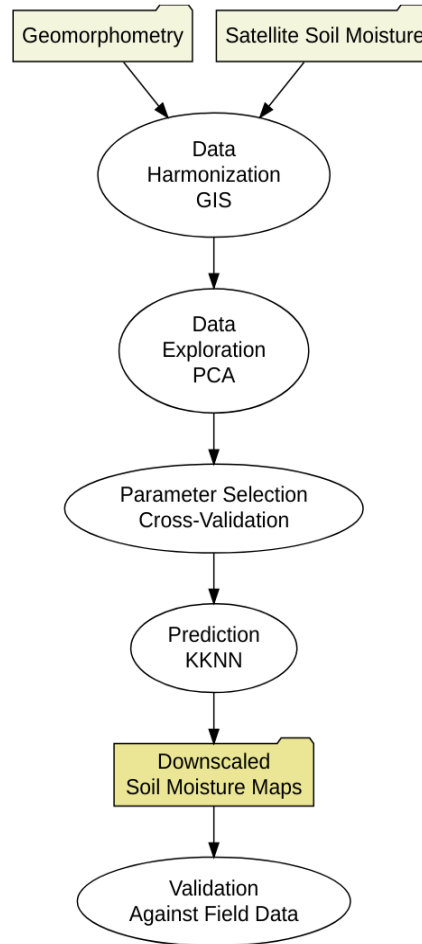
## 136 **Materials and Methods**

137 Our downscaling approach relied on a Digital Elevation Model (DEM), and satellite soil  
138 moisture records. Soil moisture information was acquired from the ESA-CCI [20-21]. The development  
139 and reliability (i.e., validation) of this remote sensing soil moisture product has been documented by  
140 previous studies [20-21, 45]. Our framework includes prediction factors for soil moisture from digital  
141 terrain analysis. These terrain predictors were derived across CONUS using 1km grids. Machine  
142 learning was used for generating soil moisture predictions (annual, 1991-2016) using as training data  
143 the satellite soil moisture estimates provided by the ESA-CCI. Field soil moisture observations from  
144 the North American Soil Moisture dataset were used for validating the soil moisture predictions based  
145 on digital terrain analysis (Figure 1).

146



147  
148  
149  
150  
151  
152  
153  
154  
155  
156  
157  
158



159 Figure 1: Soil moisture prediction framework. The folders are the inputs and outputs and the ovals are  
160 methods for data preparation (data bases harmonization), modeling (for prediction) and validation (for  
161 assessing the reliability of soil moisture maps).

162

### 163 Datasets and data preparation

164 We downscaled the ESA-CCI satellite soil moisture estimates between 1991 and 2016 and  
165 validated the downscaled information with field measurements (Supplementary Figure S1). The ESA-  
166 CCI soil moisture product has a daily temporal coverage from 1978 to 2016 and a spatial resolution of  
167 ~27 km (Supplementary Figure S2). Among several remotely sensed soil moisture products [16, 46-  
168 50], we decided to use the ESA-CCI soil moisture product because it covers a larger period of time

169 compared with other satellite soil moisture products (e.g., NASA SMAP). We highlight that satellite  
170 soil moisture information is used for training a machine learning model for each year, and independent  
171 field soil moisture records are only used for validating the downscaled soil moisture predictions.

172 For externally validating, we used the NASMD because it has been curated following a strict  
173 quality control calibrated for CONUS [44] (Supplementary Figure S1). This data collection effort  
174 consists of a harmonized and quality-controlled soil moisture dataset with contributions from over 2000  
175 meteorological stations across CONUS described by Quiring and colleagues [44]. The NASMD also  
176 include records of soil moisture registered in the International Soil Moisture Network (ISMN) [44, 51].  
177 The NASMD (unlike the ISMN) provides processed data from each station location in each network  
178 [44-19]. We used soil moisture records at 5 cm of depth ( $n = 5541$  daily measurements) from 668  
179 stations with available soil moisture estimates at this depth because radar-based soil moisture estimates  
180 are representative for these first few centimeters of topsoil surface [16].

181 As prediction factors for soil moisture, we calculated hydrologically meaningful terrain  
182 parameters for CONUS using information from a radar-based DEM [52-53]. These terrain parameters  
183 are quantitative spatial grids representing the topographic variability that directly influence the water  
184 distribution across the landscape [35], which supports the physical link between soil moisture and  
185 topography. These parameters were the basis for downscaling satellite soil moisture records to 1km  
186 grids. This spatial resolution captures the major variability of topographic features across CONUS and  
187 is commonly used on large-scale ecosystem studies and soil mapping efforts [53-54].

188 For the calculation of soil moisture prediction factors, we used automated digital terrain  
189 analysis using the System for Automated Geographical Analysis-Geographical Information System  
190 (SAGA-GIS) [36]. The automated implementation of SAGA-GIS for Geomorphometry (module for  
191 basic terrain analysis) includes a preprocessing stage to remove spurious sinks and reduce the presence

192 of other artifacts in the elevation gridded surface (e.g., false pikes or flat areas). After preprocessing the  
193 DEM, 15 hydrologically meaningful terrain parameters were generated for the CONUS from elevation  
194 data including primary (i.e., slope, aspect) and secondary parameters (i.e., cross-sectional curvature,  
195 longitudinal curvature, analytical hill-shading, convergence index, closed depressions, catchment area,  
196 topographic wetness index, length-slope factor, channel network base level, vertical distance to channel  
197 network, and valley depth index; Figure 2). The values of these terrain parameters (Supplementary  
198 Table S1) were harmonized with the ESA-CCI soil moisture values using as reference the central  
199 coordinates of the coarse soil moisture grids (Figure 1 *inputs*; see section 2.3).

200

## 201 Data exploration

202 We used a principal component analysis (PCA) prior to modeling for data exploration and  
203 description of general relationships between soil moisture values and topography (represented by the  
204 aforementioned terrain parameters). The purpose was to simplify the dimensionality of the data set to  
205 identify the main relationships (between soil moisture and topographic parameters) driving our  
206 downscaling framework (Figure 1 *methods*). The PCA was implemented as in previous work [55],  
207 based on a reference value representing the 0.95-quantile of the variability obtained by randomly  
208 simulating 300 data tables of equivalent size on the basis of a normal distribution. This analysis was  
209 applied to the terrain parameters at the locations of the field stations in order to compare the  
210 relationship of the first PCA and the values of soil moisture from the ESA-CCI grids and from the field  
211 data.

212

## 213 Model building

214 For this analysis we built a model for each downscaled soil moisture map. We used a machine  
215 learning kernel-based model (kernel weighted nearest neighbors, kkn) [56-57] to downscale satellite  
216 soil moisture (Figure 1 *methods*). The training dataset for each model/year were the annual values of  
217 the ESA-CCI soil moisture product. The kkn model has two main model parameters: the optimum  
218 number of neighbors ( $k$ ) and the optimal kernel function ( $okf$ ). First, we defined  $k$ , which is the number  
219 of neighbors to be considered for the prediction. Second, we selected the  $okf$ , which is a reference (e.g.,  
220 triangular, epanechnikov, Gaussian, optimal) for the probability density function of the variable to be  
221 predicted. The  $okf$  is used to convert distances (i.e., Minkowski distance) into weights used to calculate  
222 the  $k$ -weighted average. These kkn model parameters ( $k$  and  $okf$ ) were selected by the means of 10-  
223 fold cross validation as previously recommended [58]. Cross-validation is a well-known re-sampling  
224 technique that divides data into 10 roughly equal subsets. For every possible parameter value (e.g.,  $k$   
225 from 1 to 50 and  $okf$  [triangular, epanechnikov, Gaussian, optimal]), 10 different models are generated,  
226 each using 90% of the data then being evaluated on the remaining 10%. To predict soil moisture  
227 information at 1 km of spatial resolution for each year (between 1991 and 2016), we selected the  
228 combination of optimal  $k$  and  $okf$  that lead to the highest correlation (between observed and predicted  
229 data) with the lowest root mean squared error (RMSE) after the cross-validation strategy. Thus, for  
230 each year we were able to predict soil moisture across 1x1 km grids (Figure 1 *outputs*).

231

232 Validation using field observations across CONUS

233 Downscaled soil moisture grids were compared against field measurements and we computed the  
234 explained variance ( $r^2$ ) using a linear fit (observed vs predicted) for each field soil moisture location.  
235 Given the relatively low density and sparse spatial distribution of field data for validating  
236 (Supplementary Figure S1), we bootstrapped the independent validation using different sample sizes

237 (from 10 to 100% of data with increments each 10%) to avoid systematic bias associated with the  
238 spatial distribution and density of field soil moisture information. We sampled ( $n = 1000$ ) repeatedly  
239 the original and the downscaled soil moisture grids aiming to identify their correlation with the  
240 aforementioned validation dataset (i.e., observed vs predicted).

241 We also computed the spatial structure (spatial autocorrelation) of the explained variance  
242 (correlation between geographical distance and variance of  $r^2$  values) for estimating an  $r^2$  map using an  
243 interpolation technique known in geostatistics as Ordinary Kriging [59]. Ordinary Kriging is a well-  
244 known method for spatial interpolation based on the spatial structure or spatial autocorrelation of the  
245 variable of interest (the  $r^2$  values between the field observations and the predicted soil moisture values).  
246 The spatial autocorrelation is defined by the relationship between geographical distances and variance  
247 of values at a given distance, and it is commonly characterized using variograms. We followed an  
248 automated variogram parameterization (the optimal selection for the variogram parameters nugget, sill  
249 and range required to perform Ordinary Kriging) proposed in previous work [60].

250 As implemented in the automap package of R [60], the initial sill is estimated as the mean of the  
251 maximum and the median values of the semi-variance. The semi-variance is defined by the variance  
252 within multiple distance intervals. For modeling the spatial autocorrelation this algorithm iterates over  
253 multiple variogram model parameters selecting the model (e.g., spherical, exponential, Gaussian) that  
254 has the smallest residual sum of squares with the sample variogram. The initial range is defined as 0.10  
255 times the diagonal of the bounding box of the data. The initial nugget is defined as the minimum value  
256 of the semi-variance. Thus, the parameters used for obtaining a continuous map showing spatial trends  
257 in the  $r^2$  were: a Gaussian (normal) model form, a nugget value of  $0.06 \text{ m}^3 \text{ m}^{-3}$ , a sill of  $0.08 \text{ m}^3 \text{ m}^{-3}$  and  
258 an approximate range of 428.7 km. This map was generated because it could provide insights about  
259 overall sources of modeling errors (e.g., environmental similarities in multiple areas showing low or

260 high explained variance) and their spatial distribution. All analyzes were performed in R [61] using  
261 public sources of data. A reproducible example (code) for generating the soil moisture predictions in  
262 1km grids is provided as Supplementary Information S1.

263

## 264 **Results**

265 The exploratory PCA showed that the first two PCs explained 33% of the total dataset variability  
266 (Supplementary Figure S3A), where the first PC explained 18% of total variability and at least five PCs  
267 were needed to explain 70% of total variability. The first PC was best correlated with elevation  
268 ( $r=0.82$ ) and with the vertical distance to channel network ( $r=0.88$ ). Elevation varied negatively with  
269 soil moisture, as well as other secondary terrain parameters such as the base level channel network  
270 elevation (distance from each pixel to the closer highest point), while the valley depth index varied  
271 positively with soil moisture (Supplementary Figure S3B). The relative slope position (indicating the  
272 dominance of flat or complex terrain) and the topographic wetness index (which indicates areas where  
273 water tends to accumulate) were also correlated with soil moisture across the first 5 PCs. Thus, multiple  
274 terrain parameters varied positively and negatively with soil moisture values (Supplementary  
275 Information S2).

276

277

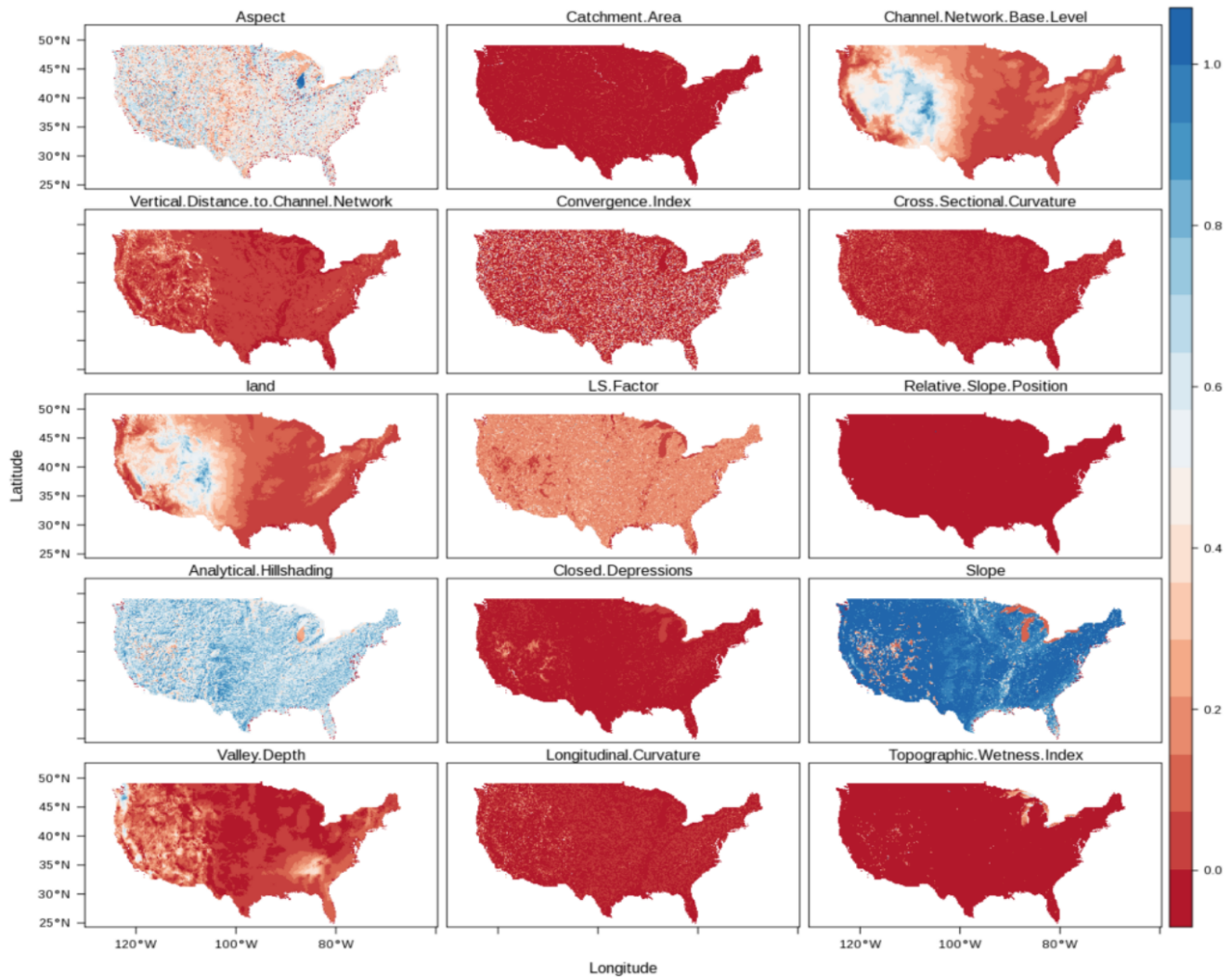
278

279

280

281

282



283

284

285 Figure 2. Elevation and hydrologically meaningful terrain parameters at 1x1km of spatial resolution  
286 derived using standard the SAGA-GIS basic terrain parameters module. These maps were normalized  
287 (between 0-1) and then used as prediction factors to downscale soil moisture across CONUS.

288

289 Our framework to predict soil moisture based on topography and remote sensing was able to  
290 explain, on average  $79 \pm 0.1\%$  of the variability of satellite soil moisture information as revealed by the

291 cross-validation strategy. The root mean squared error (RMSE) derived from the cross-validation  
292 varied around 0.03 m<sup>3</sup>/m<sup>3</sup>, while the percentage of explained variance was in all cases above 70%  
293 (Table 1).

294

295 Table 1. The cross-validation results for each year. This table shows the correlation, root mean squared  
296 error (RMSE), the number of training data available (n), the optimal kernel function (okf), and the  
297 optimal number of neighbors used for predicting to new data (k).

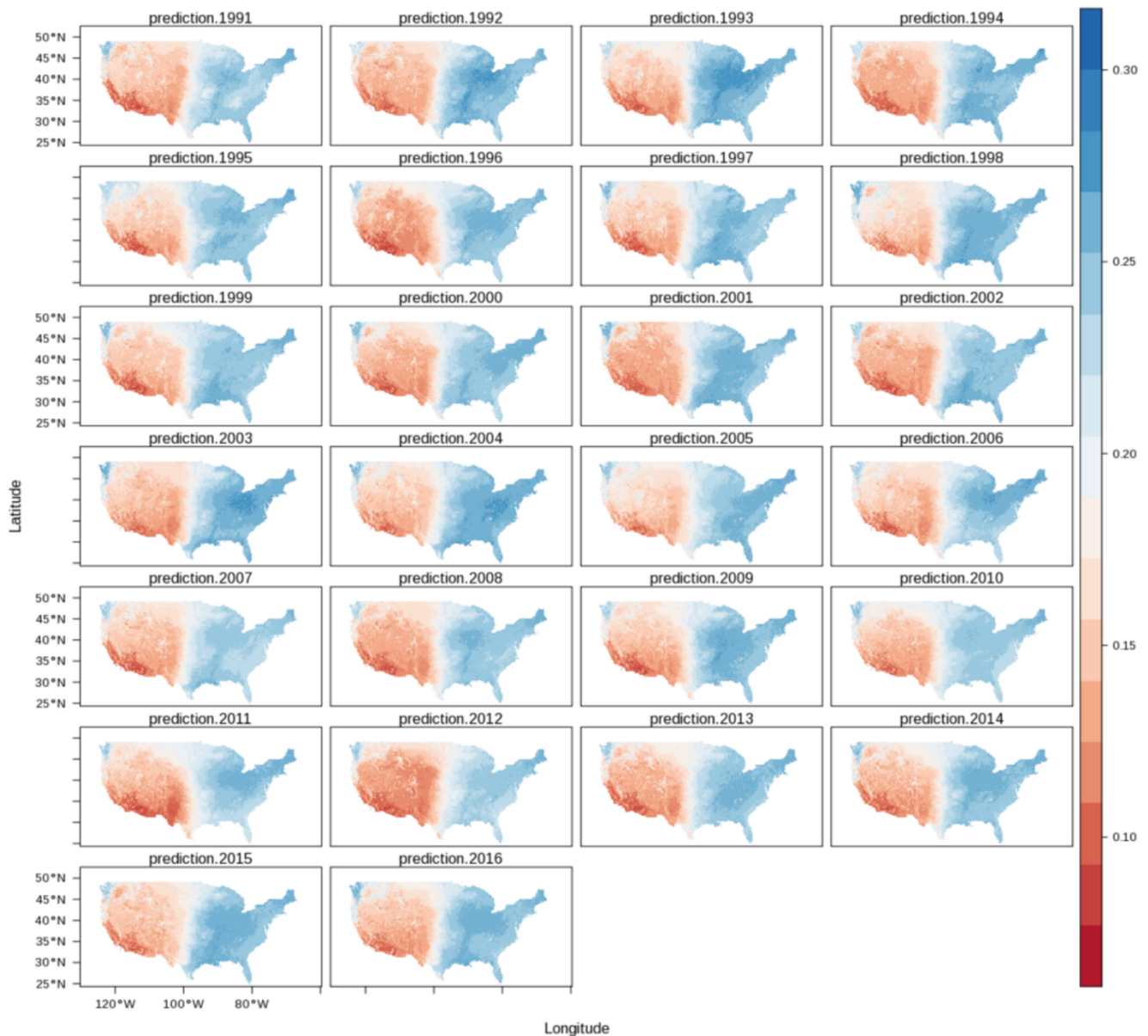
| Model | Year | Correlation | RMSE | n     | okf        | k  |
|-------|------|-------------|------|-------|------------|----|
| 1     | 1991 | 0.85        | 0.03 | 18058 | triangular | 18 |
| 2     | 1992 | 0.89        | 0.03 | 18429 | triangular | 16 |
| 3     | 1993 | 0.88        | 0.03 | 18107 | triangular | 18 |
| 4     | 1994 | 0.9         | 0.03 | 18367 | triangular | 16 |
| 5     | 1995 | 0.88        | 0.03 | 18385 | triangular | 18 |
| 6     | 1996 | 0.9         | 0.03 | 18454 | triangular | 15 |
| 7     | 1997 | 0.88        | 0.03 | 18428 | triangular | 15 |
| 8     | 1998 | 0.88        | 0.03 | 18540 | triangular | 16 |
| 9     | 1999 | 0.89        | 0.03 | 18542 | triangular | 15 |
| 10    | 2000 | 0.9         | 0.03 | 18547 | triangular | 15 |
| 11    | 2001 | 0.9         | 0.03 | 18523 | triangular | 15 |
| 12    | 2002 | 0.9         | 0.03 | 19170 | triangular | 16 |
| 13    | 2003 | 0.89        | 0.03 | 19132 | triangular | 16 |
| 14    | 2004 | 0.89        | 0.03 | 18934 | triangular | 16 |
| 15    | 2005 | 0.89        | 0.03 | 19132 | triangular | 16 |
| 16    | 2006 | 0.9         | 0.03 | 19131 | triangular | 16 |
| 17    | 2007 | 0.88        | 0.03 | 19142 | triangular | 16 |
| 18    | 2008 | 0.9         | 0.03 | 19136 | triangular | 16 |
| 19    | 2009 | 0.9         | 0.03 | 19142 | triangular | 16 |
| 20    | 2010 | 0.88        | 0.03 | 19245 | triangular | 18 |



|    |      |      |      |       |            |    |
|----|------|------|------|-------|------------|----|
| 21 | 2011 | 0.9  | 0.03 | 19255 | triangular | 18 |
| 22 | 2012 | 0.9  | 0.03 | 19252 | triangular | 16 |
| 23 | 2013 | 0.89 | 0.03 | 19226 | triangular | 16 |
| 24 | 2014 | 0.89 | 0.03 | 19227 | triangular | 16 |
| 25 | 2015 | 0.88 | 0.03 | 19231 | triangular | 16 |
| 26 | 2016 | 0.88 | 0.03 | 19225 | triangular | 16 |

298

299 By applying the model coefficients to the topographic prediction factors across CONUS, we  
300 generated 26 cross-validated maps (for years 1991-2016) of mean annual soil moisture estimates in  
301 1x1km grids (Figure 3). The downscaled product shows a higher level of spatial variability due the  
302 increased spatial detail achieved by downscaling soil moisture to 1x1km grids (Supplementary Figure  
303 S4). Our predictions reveal a clear bimodal distribution of soil moisture values (e.g., from the east to  
304 the west, Figure 4) which is also evident in the original estimate (Supplementary Figure S5). The  
305 statistical comparison (squared correlation) between the original product and the downscaled product  
306 suggests a high level of agreement showing an  $r^2$  value of 0.72.



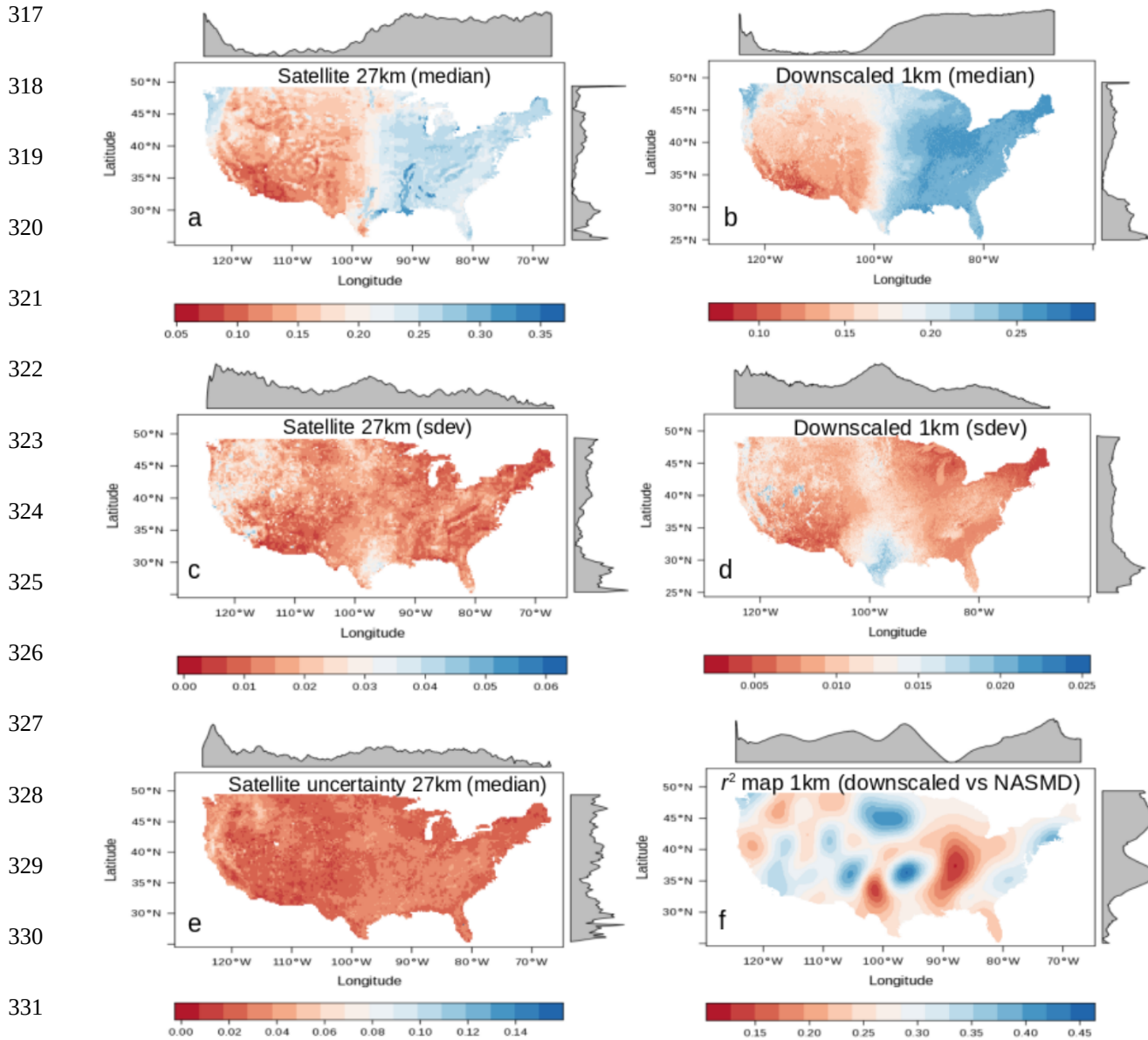
307

308 Figure 3. Annual means of soil moisture (1991-2016) downscaled to 1x1km grids across CONUS using  
309 terrain parameters as prediction factors.

310

311 We provided a visual comparison between the original satellite estimate and the downscaled  
312 results including both median and standard deviation values (Figure 4). We also show the uncertainty  
313 of the original soil moisture product as reported by its developers and the  $r^2$  map from the validation

314 against field stations. The  $r^2$  map shows the lowest values across the Central Plains of the US and the  
315 lower Mississippi basin. The lower values in the  $r^2$  map are consistent with the high uncertainty values  
316 of the original satellite estimate (Figure 4).



332

333 Figure 4. Comparison of the original and the downscaled soil moisture products. Median (a, b) and  
334 standard deviation (c, d, sdev) values of satellite soil moisture and downscaled soil moisture values

335 (1991-2016). We show the uncertainty reported by the ESA-CCI soil moisture (e) and the explained  
336 variance map ( $r^2$ ) between field data and downscaled soil moisture (f).

337

338

339 The  $r^2$  map provided insights about the relationship between soil moisture gridded surfaces and  
340 soil moisture field data. Higher  $r^2$  values were found across the east coast, the Northern Plains and  
341 water-limited environments across the western states. We found that our soil moisture downscaled  
342 output better correlates (nearly 25% improvement) with NASMD field observations when compared to  
343 the original soil moisture satellite estimates (Figure 5).

344

345

346

347

348

349

350

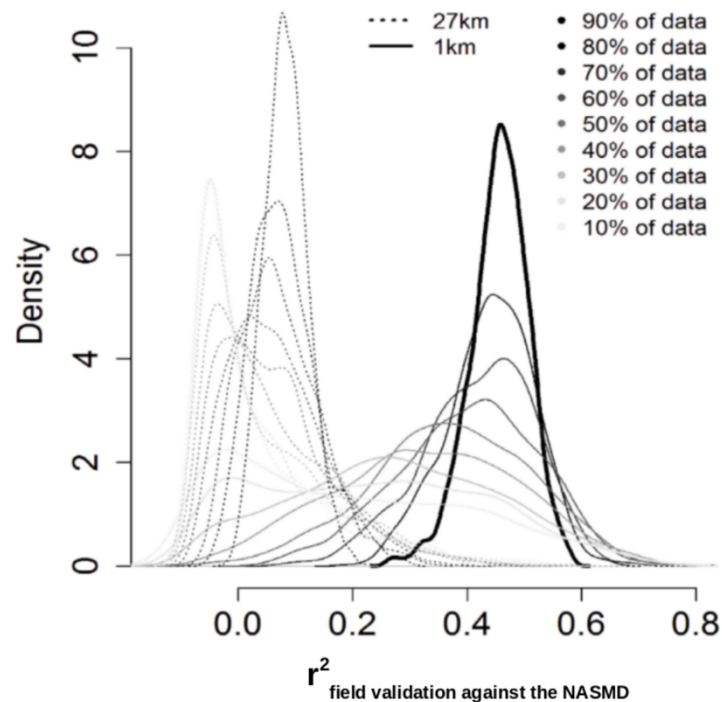
351

352

353

354

355



356 Figure 5. Validation of soil moisture gridded estimates (original 27 and 1km grids)

357 against NASMD field observations. Dashed line represents the relationship of field stations and soil  
358 moisture gridded estimates at 27x27km, while black line represents the relationship between field  
359 stations and the downscaled 1x1km soil moisture product. In all cases (all sample sizes), the 1x1km  
360 product showed higher  $r^2$  with the NASMD than the ESA-CCI soil moisture estimates.

361

362 This improvement was consistent after repeating it using random samples and different sample  
363 sizes (from 10 to 90 % of available validation data) from the NASMD field observations (Figure 5).  
364 However, there is a sparse distribution of validation data and large areas of CONUS lack of field  
365 information for validating/calibrating soil moisture predictions (Figure 6). Considering the quality-  
366 controlled records available from the NASMD across CONUS and the coarse scale of the ESA-CCI  
367 soil moisture product, our approach suggests an improvement in the spatial resolution (from 27 to 1km  
368 grids) of soil moisture estimates while maintaining the integrity of the original satellite values.

369

370

371

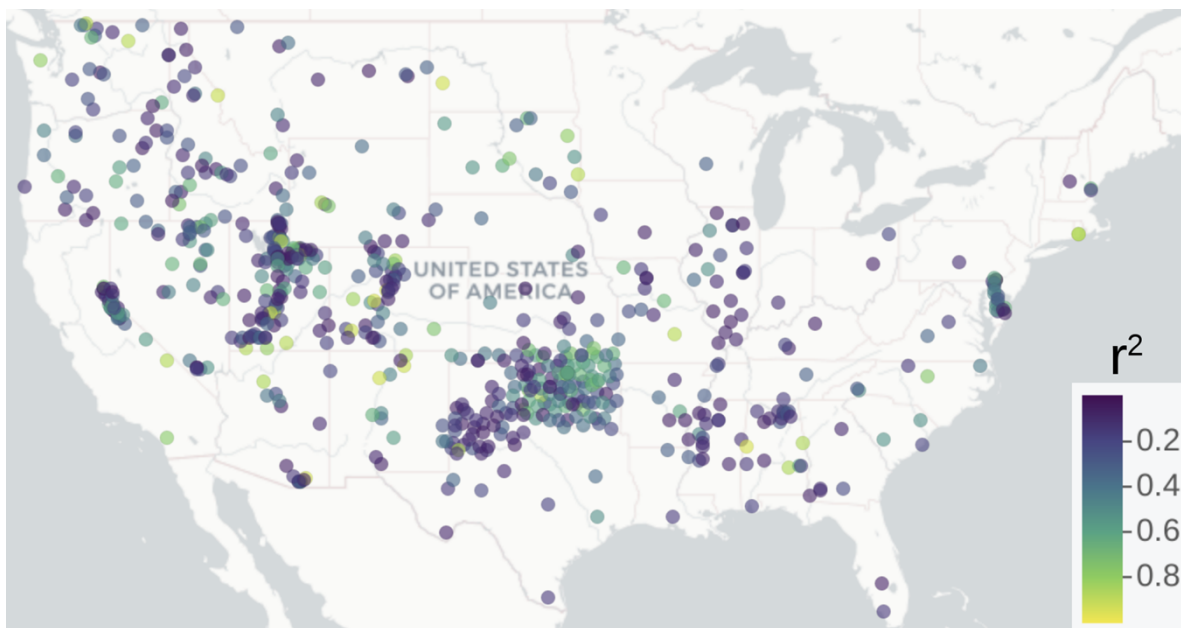
372

373

374

375

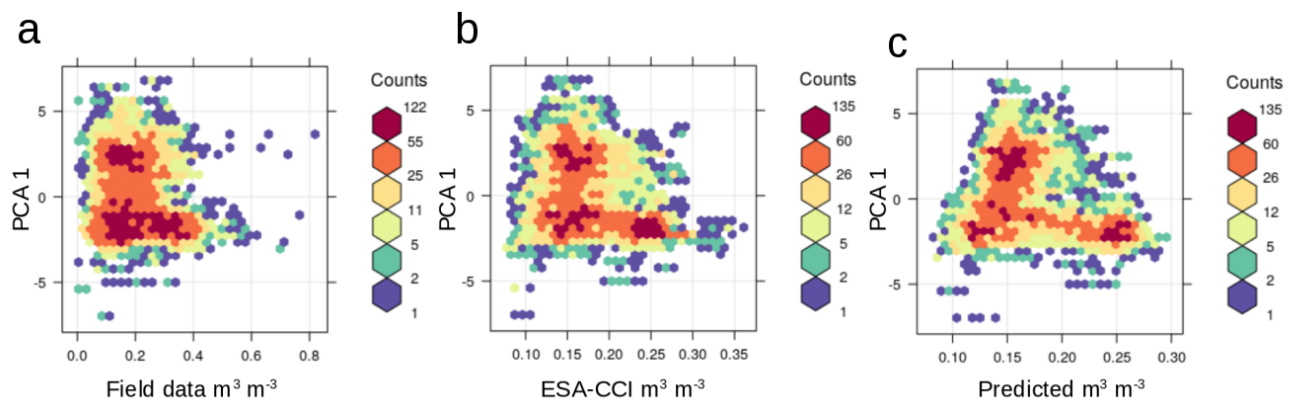
376



377 Figure 6 Explained variances computed for each meteorological station of the NASMD and the  
378 corresponding pixel of our soil moisture predictions based on geomorphometry.

379

380 The original satellite values, the downscaled product and the ISMN dataset showed a similar  
381 correlation with the terrain predictors. For example, the first PCA (represented by the distance to  
382 channel network and elevation), was negatively correlated with field soil moisture, the satellite original  
383 product and our soil moisture predictions. The correlation values were  $r=-0.17$ ,  $r=-0.27$ , and  $r=-0.28$   
384 respectively. These relationships showed a similar pattern in the statistical space (Figure 7).



385

386 Figure 7 Relationships between the first PC of terrain parameters with soil moisture field data (a), with  
387 the ESA-CCI satellite product (b), and with the soil moisture predictions based on terrain parameters  
388 (c).

389

390

## 391 Discussion

392 Our soil moisture downscaling framework was able to improve the spatial detail of ESA-CCI  
393 satellite soil moisture product and its agreement with field soil moisture records from the NASMD. It  
394 is well known that topography has a direct influence on the overall water distribution across the  
395 landscape [38-39] and in the angle between satellite retrieval and the earth's surface. Thus, we

396 demonstrated how a coarse scale satellite-based soil moisture product (27x27km of spatial resolution),  
397 in combination with hydrologically meaningful terrain parameters, can be coupled using machine  
398 learning algorithms to generate a fine-gridded and gap-free soil moisture product at the annual scale  
399 across CONUS. We found a correlation between field soil moisture estimates and topography that is  
400 similar to the correlation between satellite estimates and topography (Figure 7), suggesting that  
401 topography can be an effective predictor for direct soil moisture measurements (i.e., from microwave  
402 remote sensing). In contrast to previous downscaling efforts using vegetation and climate information  
403 [33, 62], we generated 26 annual soil moisture predictions (1991-2016, 1x1 km of spatial resolution)  
404 that are independent of ecological data (i.e., vegetation greenness) and climate information, (i.e.,  
405 precipitation and temperature). This topography-based approach has the advantage that our soil  
406 moisture output could be further related to independent datasets of ecological or climate variables [63-  
407 64]. Therefore, we provided an alternative (topography-based) approach to predict the satellite soil  
408 moisture patterns across finer spatial grids and in areas where no satellite soil moisture is available.

409         The downscaling process of satellite soil moisture from 27 to 1km grids across CONUS is  
410 supported on both internal (Table 1) and independent (Figure 5) validation frameworks to describe  
411 modeling performance. Similar results have been found recently for specific study sites [65]. These  
412 values showed explained variances >70% and RMSE values considerably below ( $\sim 0.03 \text{ m}^3 \text{ m}^{-3}$ ) the  
413 satellite soil moisture mean of  $0.22 \text{ m}^3 \text{ m}^{-3}$ , which is suitable for many applications [62], such as the  
414 detection of irrigation signals [66]. Our results obtained by the cross-validation strategy and ground  
415 validation supports the application of a topography-based model to predict satellite soil moisture  
416 estimates (Figure 4).

417         Our results showed that higher soil moisture values could be found across lower elevations, areas  
418 with generally large and gentle slopes mainly across valley bottoms and across catchment areas where

419 water tends to accumulate. This interpretation could explain the short distance in the multivariate  
420 analysis of satellite soil moisture estimates to elevation and derived terrain parameters such as the  
421 vertical distance (of each pixel) to the nearest channel network, the valley depth index and the  
422 topographic wetness index. The multivariate analysis also suggested some degree of statistical  
423 redundancy between the topographic prediction factors (Supplementary Information S2) as they were  
424 derived from the digital elevation model by the means of geomorphometry [34-39]. For example, we  
425 found that the topographic wetness index is highly correlated with the length-slope factor (>0.80%),  
426 and this is because they are two secondary parameters that depend on slope [35]. Elevation and slope  
427 are respectively required for calculating the valley depth index and the topographic wetness index [36]  
428 and these terrain parameters varied closely with soil moisture in the multivariate space (Supplementary  
429 Information S2). Thus, understanding the main relationships between topographic prediction factors  
430 and soil moisture can be useful for reducing modeling complexity while increasing our capacity to  
431 interpret modeling results.

432         The spatial detail of soil moisture estimates using 1km grids across the continental scale of  
433 CONUS is consistent with the variability of soil moisture patterns between the western and eastern  
434 United States. While drought scenarios have been recently reported for the western states [67] evidence  
435 of precipitation increase has been reported recently in the eastern states [68]. Our soil moisture  
436 downscaled estimates (Figure 3) revealed a soil moisture gradient across the Central Plains of CONUS  
437 and a clear separation of two major soil moisture data populations (i.e., soil moisture values with a  
438 bimodality distribution) from the drier west, to the humid east (Supplementary Figure S5).

439         The original satellite soil moisture estimates also show this bimodal distribution but with a lesser  
440 extent (Supplementary Figure S2). The bimodal distribution of soil moisture could be explained by a  
441 negative soil moisture and precipitation feedback in the western CONUS and a positive soil moisture



442 and precipitation feedback in the eastern CONUS [64]. Furthermore, areas with soil moisture  
443 bimodality have been recognized across global satellite observations and climate models [69]. We  
444 identified areas of low agreement between our soil moisture predictions and field stations (lower  $r^2$   
445 values) across the transitional ecosystems (Figure 4) from drier to humid soil moisture environments  
446 (i.e., Central Plains and lower Mississippi basin). It is likely that these transitional areas drive changes  
447 in water availability in surface and subsurface hydrological systems [70]. The lower Mississippi basin,  
448 specifically the area across the surroundings of the Mississippi delta, is an example of a transitional  
449 area experiencing aquifer depletion [71] where both flooding events and droughts tend to occur within  
450 shorter distances that are not captured by the original satellite soil moisture information. These are the  
451 type areas where we found lower values of agreement ( $r^2$  values) between satellite and ground soil  
452 moisture observations. These low correlation values can be also explained by the use of multiple soil  
453 moisture networks with different types of sensors and measurement techniques [19]. Also, the  
454 imperfections of prediction factors used for soil moisture spatial variability models represent a potential  
455 source of uncertainty.

456       As any downscaling effort dependent on covariates (i.e., terrain parameters), our approach is  
457 vulnerable to data quality limitations such as the presence of systematic errors on these covariates.  
458 Other errors are derived from input data imperfections and difficulties meeting modeling assumptions.  
459 These errors in soil moisture modeling inputs increase the risk of bias and uncertainty propagation to  
460 subsequent soil moisture modeling outputs and soil mapping applications [72-74]. For example,  
461 elevation data surfaces derived from remote sensing data (such as the global DEM used here) could  
462 show artifacts (i.e., false pikes or spurious sinks) due to data saturation or signal noise that can be  
463 propagated to final soil moisture predictions [75]. We minimized this issue by using SAGA-GIS [36] as  
464 it has adopted methods for preprocessing and perform DEM quality checks [76] before deriving the

465 topographic prediction factors used in this study. Because input covariates could not be fully free of  
466 errors, we advocate for reporting information on bias and  $r^2$  values to inform about accuracy (Table 1)  
467 as important components for interpreting soil moisture predictions.

468 Our results suggest that the original coarse scale soil moisture product and the values of soil  
469 moisture from the NASMD (Figure 5) are difficult to compare in terms of spatial variability, as is  
470 highlighted in previous studies [19]. This is because a satellite soil moisture pixel from the ESA-CCI  
471 product provides a value across a larger area (27x27km) than a field measurement at a specific  
472 sampling location (defined by geographical coordinates). This scale dependent effect (27x27km vs 1:1  
473 field scale) is reduced (>25%) with soil moisture predictions across finer grids (1km). The downscaled  
474 soil moisture maps showed a higher agreement with field soil moisture records from the NASMD  
475 (Figure 5), supporting the applicability of this soil moisture product for applications that required  
476 higher spatial resolution.

477 Our soil moisture predictions across 1km grids suggest that topography can be effectively used  
478 to improve the spatial detail and accuracy of satellite soil moisture estimates. Several studies have  
479 highlighted differences in spatial representativeness between ground-based observations and satellite  
480 soil moisture products [73, 77]. Other studies have shown that the spatial representativeness of the  
481 ESA-CCI soil moisture compared with field observations is higher from regional-to-continental scales  
482 than from ecosystem-to-landscape scales [78-79]. Therefore, large uncertainties of soil moisture spatial  
483 patterns (below 1km grids) needs to be resolved for assessing and better understanding the local  
484 variability of soil moisture trends. We argue that currently there is an increasing availability of high-  
485 quality digital elevation data sources with high levels of spatial resolution (e.g., 1-2 to 30 to 90m grids)  
486 across large areas of the world [80-81] that can be used to derive reliable hydrologically meaningful  
487 terrain parameters for predicting soil moisture. The relationship of these terrain parameters and field

488 soil moisture (i.e., meteorological stations) is similar to the relationship between terrain parameters and  
489 satellite soil moisture gridded estimates (Figure 7).

490 From a single information source (a remotely sensed DEM), we downscaled satellite records of  
491 soil moisture using a framework that theoretically is reproducible across multiple scales. The ultimate  
492 goal of reducing the multiple information sources for predicting soil moisture is to reduce the statistical  
493 redundancy in further modeling efforts (i.e., land carbon uptake models) and large-scale ecosystem  
494 studies (i.e., ecological niche modeling) that combine similar prediction factors for soil moisture (i.e.,  
495 climate or vegetation indexes). These include models estimating water evapotranspiration trends [82]  
496 and process based global carbon models that could also benefit from more accurate and independent  
497 soil moisture inputs [74]. To improve the spatial representativeness of satellite soil moisture estimates,  
498 the number of studies developing new downscaling approaches based on prediction factors is rapidly  
499 expanding [26, 28, 62, 83]. There is a pressing need to solve the current uncertainty of soil moisture  
500 estimates to accurately understand how soil moisture is limiting the primary productivity of terrestrial  
501 ecosystems [6]. Therefore, our results provide an alternative applicable to continental scales for  
502 downscaling satellite soil moisture estimates based on hydrologically meaningful terrain parameters.

503 The novelty of this approach is that it could be applicable to multiple temporal resolutions (e.g.,  
504 monthly or daily) as it generates independent models for each period of interest and at multiple spatial  
505 scales as the availability of terrain parameters for modeling purposes has increased substantially (i.e.,  
506 meters) in the last decade. Increasing the temporal resolution of downscaled maps (i.e., from yearly to  
507 monthly predictions) is beyond the scope of this study, will increase computational costs, but are  
508 theoretically possible following this approach. While monthly or weekly (or even daily soil moisture  
509 datasets) are valuable sources for large scale earth system modeling, yearly averages are also valuable  
510 for detecting long term trends in the climate-land system. Rather than focusing on temporal variability

511 of soil moisture, our results provide insights for improving the spatial variability and consequently the  
512 spatial representation of soil moisture gridded surfaces derived from satellite information.

513

## 514 **Conclusion**

515       Recent studies highlight the necessity of detailed soil moisture products to account for soil  
516 moisture limitation in terrestrial ecosystems. We developed a geomorphometry-based framework to  
517 couple satellite soil moisture records with hydrologically meaningful terrain parameters. We predicted  
518 (i.e., downscaled) soil moisture using 1x1km grids across CONUS at a yearly scale from 1991 to 2016.  
519 This gap-free soil moisture product improved the spatial detail of the original satellite soil moisture  
520 grids and the overall agreement (increased by >20%) of these grids with the NASMD field soil  
521 moisture records. Our findings suggest that digital terrain analysis can be applied to elevation data  
522 sources to derive hydrologically meaningful terrain parameters and use these parameters predict soil  
523 moisture spatial patterns. Our framework is reproducible across the world because it is based on  
524 publicly available DEMs, ground and satellite soil moisture data.

525

526

## 527 **Acknowledgments**

528 MG acknowledges a fellowship from CONACyT. RV acknowledges support from the National Science  
529 Foundation CIF21 DIBBs (Grant #1724843).

530

## 531 **Author Contributions**

532 **Conceptualization:** Mario Guevara, Rodrigo Vargas

533 **Data curation:** Mario Guevara

534 **Formal analysis:** Mario Guevara

535 **Writing – original draft:** Mario Guevara

536 **Writing – review & editing:** Rodrigo Vargas

537

538

## 539 **References**

- [1] Greve, P., Gudmundsson, L., Seneviratne, S.I., 2018. Regional scaling of annual mean precipitation and water availability with global temperature change. *Earth Syst. Dynam.* 9, 227–240. <https://doi.org/10.5194/esd-9-227-2018>
- [2] Seneviratne, S.I., Corti, T., Davin, E.L., Hirschi, M., Jaeger, E.B., Lehner, I., Orlowsky, B., Teuling, A.J., 2010. Investigating soil moisture–climate interactions in a changing climate: A review. *Earth-Science Reviews* 99, 125–161. <https://doi.org/10.1016/j.earscirev.2010.02.004>
- [3] Seneviratne, S.I., Wilhelm, M., Stanelle, T., van den Hurk, B., Hagemann, S., Berg, A., Cheruy, F., Higgins, M.E., Meier, A., Brovkin, V., Claussen, M., Ducharne, A., Dufresne, J.-L., Findell, K.L., Ghattas, J., Lawrence, D.M., Malyshev, S., Rummukainen, M., Smith, B., 2013. Impact of soil moisture–climate feedbacks on CMIP5 projections: First results from the GLACE-CMIP5 experiment: GLACE-CMIP5 EXPERIMENT. *Geophysical Research Letters* 40, 5212–5217. <https://doi.org/10.1002/grl.50956>
- [4] Western, A.W., Grayson, R.B., Blöschl, G., Willgoose, G.R., McMahon, T.A., 1999. Observed spatial organization of soil moisture and its relation to terrain indices. *Water Resour. Res.* 35, 797–810. <https://doi.org/10.1029/1998WR900065>
- [5] Dorigo, W., Wagner, W., Albergel, C., Albrecht, F., Balsamo, G., Brocca, L., Chung, D., Ertl, M., Forkel, M., Gruber, A., Haas, E., Hamer, P.D., Hirschi, M., Ikonen, J., de Jeu, R., Kidd, R., Lahoz, W., Liu, Y.Y., Miralles, D., Mistelbauer, T., Nicolai-Shaw, N., Parinussa, R., Pratola, C., Reimer, C., van der Schalie, R., Seneviratne, S.I., Smolander, T., Lecomte, P., 2017. ESA CCI Soil Moisture for improved Earth system understanding: State-of-the art and future directions. *Remote Sensing of Environment, Earth Observation of Essential Climate Variables* 203, 185–215. <https://doi.org/10.1016/j.rse.2017.07.001>

- [6] Stocker, B. D., Zscheischler, J., Keenan, T. F., Prentice, I. C., Peñuelas, J., & Seneviratne, S. I. 2018. Quantifying soil moisture impacts on light use efficiency across biomes. *New Phytol.*, 218(4), 1430–1449. doi: 10.1111/nph.15123
- [7] Brocca, L., Ciabatta, L., Massari, C., Camici, S., & Tarpanelli, A. 2017. Soil Moisture for Hydrological Applications: Open Questions and New Opportunities. *Water*, 9(2), 140. doi: 10.3390/w9020140
- 540 [8] Vargas, R., Sánchez-Cañete, P., Serrano-Ortiz, P., Curiel Yuste, J., Domingo, F., López-  
541 Ballesteros, A. and Oyonarte, C., 2018. Hot-moments of soil CO<sub>2</sub> efflux in a water-limited  
542 grassland. *Soil Systems*, 2(3), p.47.
- 543 [9] Asner, G.P., Alencar, A., 2010. Drought impacts on the Amazon forest: the remote sensing  
544 perspective. *New phytologist*.
- 545 [10] Cook, B.D., Corp, L.A., Nelson, R.F., Middleton, E.M., Morton, D.C., McCorkel, J.T., Masek,  
546 J.G., Ranson, K.J., Ly, V., Montesano, P.M., 2013. NASA Goddard’s LiDAR, Hyperspectral and  
547 Thermal (G-LiHT) Airborne Imager. *Remote Sensing* 5, 4045–4066.  
548 <https://doi.org/10.3390/rs5084045>
- 549 [11] Dai, A., 2011. Drought under global warming: a review. *Wiley Interdisciplinary Reviews:*  
550 *Climate Change* 2, 45–65. <https://doi.org/10.1002/wcc.81>
- [12] Samaniego, L., Thober, S., Kumar, R., Wanders, N., Rakovec, O., Pan, M., Zink, M., Sheffield, J., Wood, E.F., Marx, A., 2018. Anthropogenic warming exacerbates European soil moisture droughts. *Nature Climate Change* 8, 421–426. <https://doi.org/10.1038/s41558-018-0138-5>
- [13] van der Molen, M.K., Dolman, A.J., Ciais, P., Eglin, T., Gobron, N., Law, B.E., Meir, P., Peters, W., Phillips, O.L., Reichstein, M., Chen, T., Dekker, S.C., Doubková, M., Friedl, M.A.,

- Jung, M., van den Hurk, B.J.J.M., de Jeu, R.A.M., Kruijt, B., Ohta, T., Rebel, K.T., Plummer, S., Seneviratne, S.I., Sitch, S., Teuling, A.J., van der Werf, G.R., Wang, G., 2011. Drought and ecosystem carbon cycling. *Agricultural and Forest Meteorology* 151, 765–773.  
<https://doi.org/10.1016/j.agrformet.2011.01.018>
- [14] Luo, Y., Ahlström, A., Allison, S.D., Batjes, N.H., Brovkin, V., Carvalhais, N., Chappell, A., Ciais, P., Davidson, E.A., Finzi, A., Georgiou, K., Guenet, B., Hararuk, O., Harden, J.W., He, Y., Hopkins, F., Jiang, L., Koven, C., Jackson, R.B., Jones, C.D., Lara, M.J., Liang, J., McGuire, A.D., Parton, W., Peng, C., Randerson, J.T., Salazar, A., Sierra, C.A., Smith, M.J., Tian, H., Todd-Brown, K.E.O., Torn, M., Groenigen, K.J., Wang, Y.P., West, T.O., Wei, Y., Wieder, W.R., Xia, J., Xu, Xia, Xu, Xiaofeng, Zhou, T., 2016. Toward more realistic projections of soil carbon dynamics by Earth system models. *Global Biogeochemical Cycles* 30, 40–56. <https://doi.org/10.1002/2015GB005239>
- [15] Walsh, B., Ciais, P., Janssens, I.A., Peñuelas, J., Riahi, K., Rydzak, F., Vuuren, D.P. van, Obersteiner, M., 2017. Pathways for balancing CO<sub>2</sub> emissions and sinks. *Nature Communications* 8, 14856. <https://doi.org/10.1038/ncomms14856>
- [16] Owe, M., Van de Griend, A.A., 1998. Comparison of soil moisture penetration depths for several bare soils at two microwave frequencies and implications for remote sensing. *Water Resources Research* 34, 2319–2327. <https://doi.org/10.1029/98WR01469>
- [17] Entekhabi, D., Yueh, S., et al., 2014. SMAP handbook—Soil Moisture Active Passive: Mapping Soil Moisture and Freeze/Thaw From Space, Jet Propulsion Lab., California Inst. Technol., Pasadena, Calif.
- [18] Singh, R.S., Reager, J.T., Miller, N.L., Famiglietti, J.S., 2015. Toward hyper-resolution land-surface modeling: The effects of fine-scale topography and soil texture on CLM4.0 simulations



over the Southwestern U.S.: Effects of fine-scale resolution on CLM4.0 in Southwest US.

Water Resources Research 51, 2648–2667. <https://doi.org/10.1002/2014WR015686>

- [19] Dirmeyer, Paul A., Jiexia Wu, Holly E. Norton, Wouter A. Dorigo, Steven M. Quiring, Trenton W. Ford, Joseph A. Santanello, et al. 2016. “Confronting Weather and Climate Models with Observational Data from Soil Moisture Networks over the United States.” *Journal of Hydrometeorology* 17 (4): 1049–67. <https://doi.org/10.1175/jhm-d-15-0196.1>.
- [20] Liu, Y.Y., Dorigo, W.A., Parinussa, R.M., de Jeu, R.A.M., Wagner, W., McCabe, M.F., Evans, J.P., van Dijk, A.I.J.M., 2012. Trend-preserving blending of passive and active microwave soil moisture retrievals. *Remote Sensing of Environment* 123, 280–297.  
<https://doi.org/10.1016/j.rse.2012.03.014>
- [21] Liu, Y.Y., Parinussa, R.M., Dorigo, W.A., De Jeu, R.A.M., Wagner, W., van Dijk, A.I.J.M., McCabe, M.F., Evans, J.P., 2011. Developing an improved soil moisture dataset by blending passive and active microwave satellite-based retrievals. *Hydrology and Earth System Sciences* 15, 425–436. <https://doi.org/10.5194/hess-15-425-2011>
- [22] McColl, K.A., Alemohammad, S.H., Akbar, R., Konings, A.G., Yueh, S., Entekhabi, D., 2017. The global distribution and dynamics of surface soil moisture. *Nature Geoscience* 10, 100–104.  
<https://doi.org/10.1038/ngeo2868>
- [23] Montzka, C., K. Rötzer, H.R. Bogaen, and H. Vereecken. 2018. A new soil moisture downscaling approach for SMAP, SMOS and ASCAT by predicting sub-grid variability. *Remote Sens.* 10(3):427. doi:10.3390/rs10030427
- [24] Afshar, M.H., Yilmaz, M.T., 2017. The added utility of nonlinear methods compared to linear methods in rescaling soil moisture products. *Remote Sensing of Environment* 196, 224–237.  
<https://doi.org/10.1016/j.rse.2017.05.017>

- [25] Jin, Y., Ge, Y., Wang, J., Heuvelink, G.B.M., Wang, L., 2018. Geographically Weighted Area-to-Point Regression Kriging for Spatial Downscaling in Remote Sensing. *Remote Sensing* 10, 579. <https://doi.org/10.3390/rs10040579>
- [26] Kearney, M.R., Maino, J.L., 2018. Can next-generation soil data products improve soil moisture modelling at the continental scale? An assessment using a new microclimate package for the R programming environment. *Journal of Hydrology* 561, 662–673. <https://doi.org/10.1016/j.jhydrol.2018.04.040>
- [27] Piles, M., Camps, A., Vall-llossera, M., Corbella, I., Panciera, R., Rudiger, C., Kerr, Y.H., Walker, J., 2011. Downscaling SMOS-Derived Soil Moisture Using MODIS Visible/Infrared Data. *IEEE Transactions on Geoscience and Remote Sensing* 49, 3156–3166. <https://doi.org/10.1109/TGRS.2011.2120615>
- [28] Ranney, K.J., Niemann, J.D., Lehman, B.M., Green, T.R., Jones, A.S., 2015. A method to downscale soil moisture to fine resolutions using topographic, vegetation, and soil data. *Advances in Water Resources* 76, 81–96. <https://doi.org/10.1016/j.advwatres.2014.12.003>
- [29] Wang, A., Zhang, M., Shi, J., Mu, T., Gong, H., Xie, C., 2012. Space-time analysis on downscaled soil moisture data and parameters of plant growth. *Transactions of the Chinese Society of Agricultural Engineering* 28, 164–169.
- [30] Yu, G., Di, L., Yang, W., 2008. Downscaling of Global Soil Moisture using Auxiliary Data. *IEEE*, pp. III-230-III–233. <https://doi.org/10.1109/IGARSS.2008.4779325>
- [31] McBratney, A., Mendonça Santos, M., Minasny, B., 2003. On digital soil mapping. *Geoderma* 117, 3–52. [https://doi.org/10.1016/S0016-7061\(03\)00223-4](https://doi.org/10.1016/S0016-7061(03)00223-4)
- [32] Bauer-Marschallinger, B., Freeman, V., Cao, S., Paulik, C., Schaufler, S., Stachl, T., ...Wagner, W. (2019). Toward Global Soil Moisture Monitoring With Sentinel-1: Harnessing Assets and

Overcoming Obstacles. IEEE Trans. Geosci. Remote Sens., 57(1), 520–539. doi:  
10.1109/TGRS.2018.2858004

- [33] Morelo B., Merlin O., Malbeteau Y., Al Bitar A., Cabot F., Stefan V., Kerr Y., Bacon S., Cosh., M., Bindlish R., Jackson T.J. 2016. SMOS disaggregated soil moisture product at 1km resolution: Processor overview and first validation results. Remote Sensing of Environment 180, 361-376 <https://doi.org/10.1016/j.rse.2016.02.045>
- [34] Pike, R.J., Evans, I.S., , T., 2009. Chapter 1 Geomorphometry: A Brief Guide, in: Developments in Soil Science. Elsevier, pp. 3–30.
- [35] Wilson, J. P., & Gallant, J. C. (2000). Digital terrain analysis. Terrain analysis: Principles and applications, 6(12), 1–27.
- [36] Conrad, O., Bechtel, B., Bock, M., Dietrich, H., Fischer, E., Gerlitz, L., Wehberg, J., Wichmann, V., Böhner, J., 2015. System for Automated Geoscientific Analyses (SAGA) v. 2.1.4. Geoscientific Model Development 8, 1991–2007. <https://doi.org/10.5194/gmd-8-1991-2015>
- [37] Wilson, J.P., 2012. Digital terrain modeling. Geomorphology, Geospatial Technologies and Geomorphological Mapping Proceedings of the 41st Annual Binghamton Geomorphology Symposium 137, 107–121. <https://doi.org/10.1016/j.geomorph.2011.03.012>
- [38] Florinsky, I.V., 2016. Chapter 9 - Influence of Topography on Soil Properties, in: Florinsky, I.V. (Ed.), Digital Terrain Analysis in Soil Science and Geology (Second Edition). Academic Press, pp. 265–270. <https://doi.org/10.1016/B978-0-12-804632-6.00009-2>
- [39] Florinsky, I.V., 2012. The Dokuchaev hypothesis as a basis for predictive digital soil mapping (on the 125th anniversary of its publication). Eurasian Soil Science 45, 445–451. <https://doi.org/10.1134/S1064229312040047>

- [40] Hengl, T., MacMillan, R.A., 2019. Predictive Soil Mapping with R. OpenGeoHub foundation, Wageningen, the Netherlands, 370 pages, [www.soilmapper.org](http://www.soilmapper.org), ISBN: 978-0-359-30635-0.
- [41] Reichstein, M., Camps-Valls, G., Stevens, B., Jung, M., Denzler, J., Carvalhais, N., & Prabhat. 2019. Deep learning and process understanding for data-driven Earth system science. *Nature*, 566(7743), 195. doi: 10.1038/s41586-019-0912-1
- [42] Warner, D.L., Guevara, M., Inamdar, S. and Vargas, R., 2019. Upscaling soil-atmosphere CO<sub>2</sub> and CH<sub>4</sub> fluxes across a topographically complex forested landscape. *Agricultural and forest meteorology*, 264, pp.80-91.
- [43] Coopersmith, E. J., Cosh, M. H., Bell, J. E., & Boyles, R. 2016. Using machine learning to produce near surface soil moisture estimates from deeper in situ records at U.S. Climate Reference Network (USCRN) locations: Analysis and applications to AMSR-E satellite validation. *Adv. Water Resour.*, 98, 122–131. doi: 10.1016/j.advwatres.2016.10.007
- [44] Quiring, S.M., Ford, T.W., Wang, J.K., Khong, A., Harris, E., Lindgren, T., Goldberg, D.W., Li, Z., 2016. The North American Soil Moisture Database: Development and Applications. *Bulletin of the American Meteorological Society* 97, 1441–1459.  
<https://doi.org/10.1175/BAMS-D-13-00263.1>
- [45] Dorigo, W., Wagner, W., Albergel, C., Albrecht, F., Balsamo, G., Brocca, L., Chung, D., Ertl, M., Forkel, M., Gruber, A., Haas, E., Hamer, P.D., Hirschi, M., Ikonen, J., de Jeu, R., Kidd, R., Lahoz, W., Liu, Y.Y., Miralles, D., Mistelbauer, T., Nicolai-Shaw, N., Parinussa, R., Pratola, C., Reimer, C., van der Schalie, R., Seneviratne, S.I., Smolander, T., Lecomte, P., 2017. ESA CCI Soil Moisture for improved Earth system understanding: State-of-the art and future directions. *Remote Sensing of Environment, Earth Observation of Essential Climate Variables* 203, 185–215. <https://doi.org/10.1016/j.rse.2017.07.001>

- [46] Bindlish, R., Jackson, T., Cosh, M., Tianjie Zhao, O'Neill, P., 2015. Global Soil Moisture From the Aquarius/SAC-D Satellite: Description and Initial Assessment. *IEEE Geoscience and Remote Sensing Letters* 12, 923–927. <https://doi.org/10.1109/LGRS.2014.2364151>
- [47] Entekhabi, D., Njoku, E.G., O'Neill, P.E., Kellogg, K.H., Crow, W.T., Edelstein, W.N., Entin, J.K., Goodman, S.D., Jackson, T.J., Johnson, J., Kimball, J., Piepmeier, J.R., Koster, R.D., Martin, N., McDonald, K.C., Moghaddam, M., Moran, S., Reichle, R., Shi, J.C., Spencer, M.W., Thurman, S.W., Tsang, L., Van Zyl, J., 2010. The Soil Moisture Active Passive (SMAP) Mission. *Proceedings of the IEEE* 98, 704–716. <https://doi.org/10.1109/JPROC.2010.2043918>
- [48] Naeimi, V., Paulik, C., Bartsch, A., Wagner, W., Kidd, R., Park, S.-E., Elger, K., Boike, J., 2012. ASCAT Surface State Flag (SSF): Extracting Information on Surface Freeze/Thaw Conditions From Backscatter Data Using an Empirical Threshold-Analysis Algorithm. *IEEE Transactions on Geoscience and Remote Sensing* 50, 2566–2582. <https://doi.org/10.1109/TGRS.2011.2177667>
- [49] Naeimi, V., Scipal, K., Bartalis, Z., Hasenauer, S., Wagner, W., 2009. An Improved Soil Moisture Retrieval Algorithm for ERS and METOP Scatterometer Observations. *IEEE Transactions on Geoscience and Remote Sensing* 47, 1999–2013. <https://doi.org/10.1109/TGRS.2008.2011617>
- [50] Wagner, W., Lemoine, G., Rott, H., 1999. A Method for Estimating Soil Moisture from ERS Scatterometer and Soil Data. *Remote Sensing of Environment* 70, 191–207. [https://doi.org/10.1016/S0034-4257\(99\)00036-X](https://doi.org/10.1016/S0034-4257(99)00036-X)
- [51] Dorigo, W.A., Wagner, W., Hohensinn, R., Hahn, S., Paulik, C., Xaver, A., Gruber, A., Drusch, M., Mecklenburg, S., van Oevelen, P., Robock, A., Jackson, T., 2011. The International Soil Moisture Network: a data hosting facility for global in situ soil moisture measurements.

Hydrology and Earth System Sciences 15, 1675–1698. <https://doi.org/10.5194/hess-15-1675-2011>

- [52] Becker, J.J., Sandwell, D.T., Smith, W.H.F., Braud, J., Binder, B., Depner, J., Fabre, D., Factor, J., Ingalls, S., Kim, S.-H., Ladner, R., Marks, K., Nelson, S., Pharaoh, A., Trimmer, R., Von Rosenberg, J., Wallace, G., Weatherall, P., 2009. Global Bathymetry and Elevation Data at 30 Arc Seconds Resolution: SRTM30\_PLUS. *Marine Geodesy* 32, 355–371. <https://doi.org/10.1080/01490410903297766>
- [53] Hengl T, de Jesus JM, MacMillan RA, Batjes NH, Heuvelink GBM, Ribeiro E, et al. SoilGrids1km — Global Soil Information Based on Automated Mapping. Bond-Lamberty B, editor. *PLoS ONE*. 2014;9: e105992. doi:10.1371/journal.pone.0105992
- [54] Tuanmu, M.-N., & Jetz, W. A global 1-km consensus land-cover product for biodiversity and ecosystem modelling. *Global Ecol. Biogeogr.*, 23(9), 1031–1045. 2014. doi: 10.1111/geb.12182
- [55] Thuleau S, and Husson F. 2018. FactoInvestigate: Automatic Description of Factorial Analysis. R package version 1.3. <https://CRAN.R-project.org/package=FactoInvestigate>
- [56] Hechenbichler, K., Schliep, K., 2006. Weighted k-nearest-neighbor techniques and ordinal classification, in: Discussion Paper 399, SFB 386.
- [57] Hechenbichler, K., Schliep, K., 2004. Weighted k-Nearest-Neighbor Techniques and Ordinal Classification [WWW Document]. URL <https://epub.ub.uni-muenchen.de/1769/> (accessed 12.24.16).
- [58] Borra, S., Di Ciaccio, A., 2010. Measuring the prediction error. A comparison of cross-validation, bootstrap and covariance penalty methods. *Computational Statistics & Data Analysis* 54, 2976–2989. <https://doi.org/10.1016/j.csda.2010.03.004>

- [59] Oliver, M. A., & Webster, R. 2014. A tutorial guide to geostatistics: Computing and modelling variograms and kriging. *CATENA*, 113, 56–69. doi: 10.1016/j.catena.2013.09.006
- [60] Hiemstra, P. H., Pebesma, E. J., Twenhöfel, C. J. W., & Heuvelink, G. B. M. 2009. Real-time automatic interpolation of ambient gamma dose rates from the Dutch radioactivity monitoring network. *Comput. Geosci.*, 35(8), 1711–1721. doi: 10.1016/j.cageo.2008.10.011
- [61] R Core Team 2018. R: A language and environment for statistical computing. R Foundation for Statistical Computing, Vienna, Austria. URL <https://www.R-project.org/>.
- [62] Colliander, A., Fisher, J. B., Halverson, G., Merlin, O., Misra, S., Bindlish, R., ...Yueh, S. 2017. Spatial Downscaling of SMAP Soil Moisture Using MODIS Land Surface Temperature and NDVI During SMAPVEX15. *IEEE Geosci. Remote Sens. Lett.*, 14(11), 2107–2111. doi: 10.1109/LGRS.2017.2753203
- [63] He, L., Chen, J. M., Liu, J., Bélair, S., & Luo, X. 2017. Assessment of SMAP soil moisture for global simulation of gross primary production. *J. Geophys. Res. Biogeosci.*, 122(7), 1549–1563. doi: 10.1002/2016JG003603
- [64] Tuttle, S. & Salvucci, G. 2016. Empirical evidence of contrasting soil moisture-precipitation feedbacks across the United States. *Science* **352**, 825–828.
- [65] Colliander, A., Jackson, T. J., Bindlish, R., Chan, S., Das, N., Kim, S. B., ...Yueh, S. 2017. Validation of SMAP surface soil moisture products with core validation sites. *Remote Sens. Environ.*, 191, 215–231. doi: 10.1016/j.rse.2017.01.021
- [66] Lawston, P. M., Santanello, J. A., & Kumar, S. V. 2017. Irrigation Signals Detected From SMAP Soil Moisture Retrievals. *Geophys. Res. Lett.*, 44(23), 11,860–11,867. doi: 10.1002/2017GL075733

- [67] Diffenbaugh, N. S., Swain, D. L., & Touma, D. 2015. Anthropogenic warming has increased drought risk in California. *Proc. Natl. Acad. Sci. U.S.A.*, 112(13), 3931–3936. doi: 10.1073/pnas.1422385112
- [68] Easterling, D. R., Kunkel, K. E., Arnold, J. R., Knutson, T., LeGrande, A. N., Leung, L. R., Wehner, M. F. 2017. Precipitation change in the United States. In D. J. Wuebbles, D. W. Fahey, K. A. Hibbard, D. J. Dokken, B. C. Stewart, & T. K. Maycock (Eds.), *Climate science special report: Fourth national climate assessment (Vol. I, pp. 207– 230)*. Washington, DC: U.S. Global Change Research Program
- [69] Vilasa L, Miralles DG, de Jeu RAM, Dolman AJ. Global soil moisture bimodality in satellite observations and climate models. *Journal of Geophysical Research: Atmospheres*. 2017;122: 4299–4311. doi:10.1002/2016jd026099
- [70] Dyer, J., & Mercer, A. 2013. Assessment of Spatial Rainfall Variability over the Lower Mississippi River Alluvial Valley. *J. Hydrometeorol.*, 14(6), 1826–1843. doi: 10.2307/24914344
- [71] Reba, M. L., Massey, J. H., Adviento-Borbe, M. A., Leslie, D., Yaeger, M. A., Anders, M., & Farris, J. 2017. Aquifer Depletion in the Lower Mississippi River Basin: Challenges and Solutions. *Journal of Contemporary Water Research & Education*, 162(1), 128–139. doi: 10.1111/j.1936-704X.2017.03264.x
- [72] Heuvelink, G.B. M., Millward, A.A., 1999. Error propagation in environmental modelling with GIS. *Cartographica* 36, 69.
- [73] Miralles, D.G., Crow, W.T., Cosh, M.H., 2010. Estimating Spatial Sampling Errors in Coarse-Scale Soil Moisture Estimates Derived from Point-Scale Observations. *Journal of Hydrometeorology* 11, 1423–1429. <https://doi.org/10.1175/2010JHM1285.1>



- [74] Munguia-Flores, F., Arndt, S., Ganesan, A. L., Murray-Tortarolo, G., & Hornibrook, E. R. C. 2018. Soil Methanotrophy Model (MeMo v1.0): a process-based model to quantify global uptake of atmospheric methane by soil. *Geosci. Model Dev.*, 11(6), 2009–2032. doi: 10.5194/gmd-11-2009-2018
- [75] Lindsay J.B, Creed I.F. Removal of artifact depressions from digital elevation models: towards a minimum impact approach. *Hydrological Processes*. 2005;19: 3113–3126. doi:10.1002/hyp.5835
- [76] Planchon, O. & F. Darboux (2001): A fast, simple and versatile algorithm to fill the depressions of digital elevation models. *Catena* 46: 159-176
- [77] Gruber, A., Dorigo, W.A., Zwieback, S., Xaver, A., Wagner, W., 2013. Characterizing Coarse-Scale Representativeness of in situ Soil Moisture Measurements from the International Soil Moisture Network. *Vadose Zone Journal* 12, 0. <https://doi.org/10.2136/vzj2012.0170>
- [78] Nicolai-Shaw, N., Hirschi, M., Mittelbach, H., Seneviratne, S.I., 2015. Spatial representativeness of soil moisture using in situ, remote sensing, and land reanalysis data: SPATIAL REPRESENTATIVENESS OF SOIL MOISTURE. *Journal of Geophysical Research: Atmospheres* 120, 9955–9964. <https://doi.org/10.1002/2015JD023305>
- [79] Vargas, R., Sonnentag, O., Abramowitz, G., Carrara, A., Chen, J.M., Ciais, P., Correia, A., Keenan, T.F., Kobayashi, H., Ourcival, J.M. and Papale, D., 2013. Drought influences the accuracy of simulated ecosystem fluxes: a model-data meta-analysis for Mediterranean oak woodlands. *Ecosystems*, 16(5), pp.749-764.
- [80] Nelson, A., Reuter, H.I., Gessler, P., 2009. Chapter 3 DEM Production Methods and Sources, in: *Developments in Soil Science*. Elsevier, pp. 65–85.

- [81] Tadono, T., Ishida, H., Oda, F., Naito, S., Minakawa, K., Iwamoto, H., 2014. Precise Global DEM Generation by ALOS PRISM. *ISPRS Annals of Photogrammetry, Remote Sensing and Spatial Information Sciences II-4*, 71–76. <https://doi.org/10.5194/isprsannals-II-4-71-2014>
- [82] Schwingshackl, C., Hirschi, M., Seneviratne, S. I., Schwingshackl, C., Hirschi, M., & Seneviratne, S. I. 2017. Quantifying Spatiotemporal Variations of Soil Moisture Control on Surface Energy Balance and Near-Surface Air Temperature. *J. Clim.* Retrieved from <https://journals.ametsoc.org/doi/full/10.1175/JCLI-D-16-0727.1>
- [83] Jin, Y., Ge, Y., Wang, J., Heuvelink, G.B.M., Wang, L., 2018. Geographically Weighted Area-to-Point Regression Kriging for Spatial Downscaling in Remote Sensing. *Remote Sensing* 10, 579. <https://doi.org/10.3390/rs10040579>